CHAPTER - VII

ELECTROCHEMCAL INVESTIGATIONS OF LINEAR POLYESTERS ON REBAR CORROSION IN SIMULATED CONCRETE PORE SOLUTION

7.1 INTRODUCTION

The issues pertaining to the corrosion of reinforced concrete structures has been internationally recognised that holds huge expenditure to overcome. Therefore demands for securing the service life, durability and structural assessment of existing infrastructures has gained enormous attention in recent years. The main cause of such deterioration can be reasoned due to the concrete embedded which is a prime factor in destroying bridges, parking garages, off-shore structures and highways. It is precise to notice that the corrosion costs too high in developed countries, where US before fifteen years has spent more than $ 6.3 billion specifically to repair and replace prestressed concrete highways due to simple corrosion process. The corrosion in reinforced steel is an unavoidable one as it is mainly triggered due to the environmental factors like temperature, humidity, chloride content, pH, interfacial voids as well as potential of steel[1,2] which plays an important role in premature failure of buildings till date. Thus it is the responsibility of stakeholders, engineers, authorities and researchers to understand the actual behaviour of an impaired structure and to estimate the remaining service period realistically. To get a detailed insight of these deterioration process, micro level studies are more important than macro scale.

Thus in general, steel bars are protected in alkaline incubator combined with coatings or inhibitors to minimize its deterioration when exposed to harsh environment carrying corrosion inducing factors like elevated temperature, relative high humidity etc., In specific, exposure to carbonation and chloride induced medium resulted in pronounced corrosion rate with decreased alkalinity thereby initiating cathode and anode reactions[3]. Such steels reinforced with concrete are widely used all around the world in civil engineering structures, highways etc., likely due to its better strength, durability and bonding ability under sustained conditions. Though the steel reinforcement makes the possibility of governing wide span buildings, the pronounced effect of chloride ions in the atmosphere stands as a primary hindering factor for the civil engineers in limiting the durability[4,5] which is evident from the failure noticed during the construction of concrete structures in coastal areas[6]. The catalytic nature of chloride induced corrosion seem to be difficult to terminate but can be minimised. The corrosion problem in reinforced concrete has been extensively investigated by ample

researchers and the foremost cost – effective solution of adding inhibitors has been formulated which can be proceeded either preventively or restoratively[7]. Prior to the detailed discussion, a glimpse of knowledge about the concrete material, steel embedded and reinforced concrete is essential.

7.1.1 Nature of concrete

An artificial mixture of fine and granular material (aggregate/filler) which is embedded within hard matrix (cement /binder) that can fill the space and glue them together is termed as concrete. Cement concrete is a widely used material mainly comprising of calcium silicates (C_3S and C_2S), calcium aluminate (C_3A) and clinker phase (C_4AF). On the other hand, pores within the concrete filled with saturated $Ca(OH)_2$ solution and other alkalines such as NaOH and KOH provide high pH to the concrete environment thereby protecting the steel embedded.

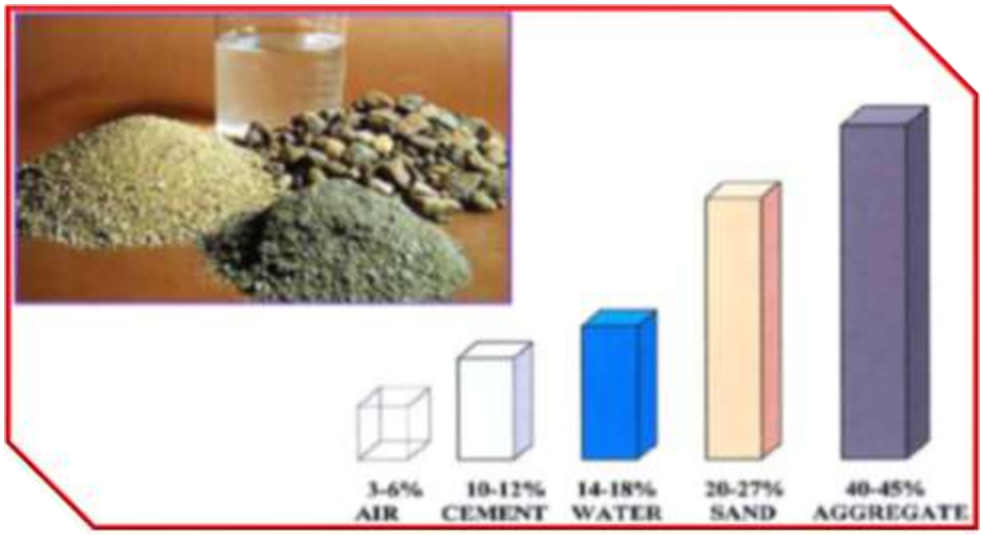

Fig. 1 Mixture of concrete

Concrete is a mixture of components as displayed in the **Fig. 1**, where the porous structure results due to cement hydration depending on water-cement ratio as well as curing temperature. Gel pores (1 to 10 nm), capillary pores (10 nm to 10 μm), macro pores and air voids (10 μm up to several mm) are the main types of pores recognised, out of which amount of capillary pores has been found to contribute more than the gel pores and air voids.

7.1.2 Nature of steel

Though the steel has a tendency to get corroded, when reinforced with concrete physico-chemical protection is favoured by the alkaline environment of the concrete medium thereby generating high pH level of 13, which is a desired level to form a thin passive oxide

layer on the metal surface to reduce the metal dissolution[8]. The inability of concrete in forming passive layer arises when the pH value of pore solution goes below 9 resulting in cracking, spalling and decreased durability of infrastructure[9,10] as shown in **Fig. 2**.

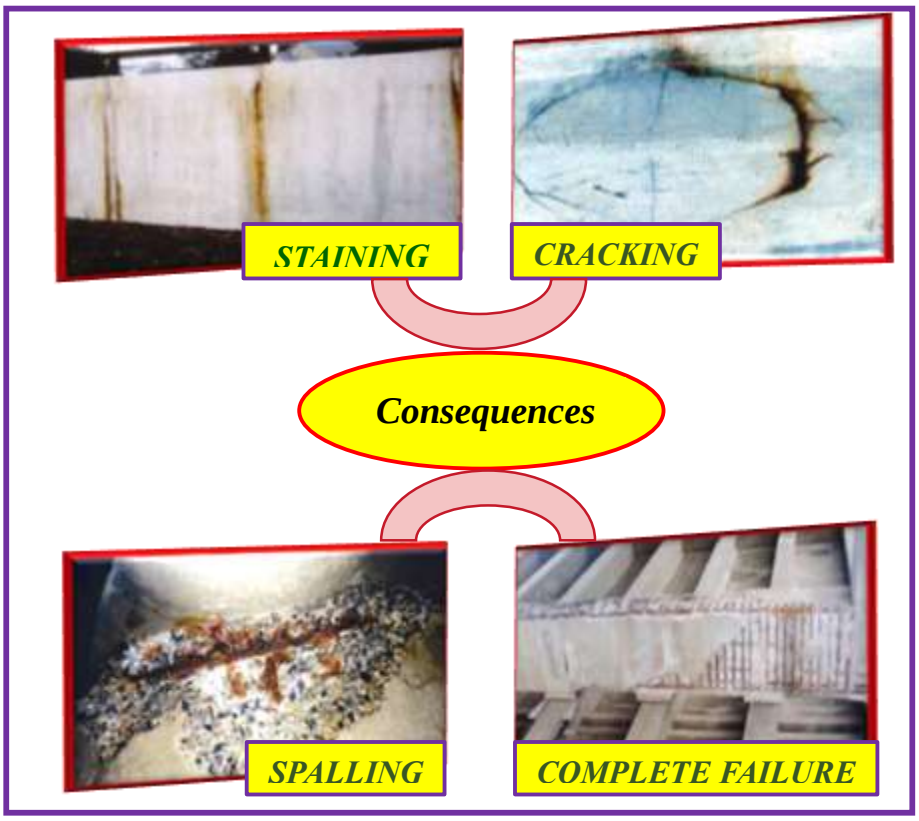

Fig. 2 Consequences of rebar corrosion

7.1.3 Reinforced corrosion

Reinforced concrete is one of the important building material due to its low cost, ease availability, versatility and prolonged durability. Such reinforced concrete suffers serious damages due to corrosion process which could not be avoided. To facilitate the reinforced corrosion, three basic parameters shown below are necessary among which absence of any one can retard the corrosion process.

- Potential difference – areas of rebar at different energy levels
- Electrolyte – concrete takes the role of electrolyte
- Metallic connection – rendered by the rebar itself

Generally the micropores of concrete rich in soluble calcium, sodium and potassium oxides forms its corresponding hydroxides when combined with water to form an alkaline environment of high passivating layer (pH 12-13) offering good protection for the steel embedded[11]. In addition, properly designed and cured concrete with low water-cement ratio

can promise for minimised corrosive attack. However the alkaline environment generated could not remain as such which could undergo deterioration in presence of aggressive ions like chloride and carbonates[12]. The transportation of these ions can follow either capillary suction or permeation or diffusion or migration process. Depending on the quality and quantity of concrete surrounding the steel bar as well as internal and external environments, breakdown of passive film can occur. Chloride ions reaching a critical level to initiate corrosion is termed as initiation period followed by propagation period where the remedial measure could be done. Based on this fact various conceptual models were proposed by various researchers[13,14] to understand the corrosion process of steel rebars. Besides various models, carbonates and chlorides are the main corrosive reagents of reinforced concrete which is explained in the forthcoming sections.

7.1.3.1 Carbonation corrosion

Carbonation corrosion is simply defined as the chemical reaction between carbon-di-oxide from the atmosphere and the hydration product of cement $Ca(OH)_2$ in concrete causing a reduction in the alkalinity of concrete thereby neutralising the pH of the pore solution from 14 to 9 and initiating the carbonation corrosion process[15],

$$Ca(OH)_2 \leftrightarrow Ca^{2+} + 2OH^-$$

Carbon dioxide dissolves in concrete pore water and forms carbonic acid before reacting with the dissolved Ca(OH)2

$$H_2O + CO_2 \leftrightarrow HCO_3^- + H^+$$

$$HCO_3^- \leftrightarrow CO_3^{2-} + H^+$$

The following neutralization reaction completes the final stage of carbonation which clearly demonstrates that $Ca(OH)_2$ which is responsible in endeavouring high pH value has been utilised.

$$Ca^{2+} + 2OH^- + 2H^+ + CO_3^{2-} \rightarrow CaCO_3 + 2H_2O$$

A condition with a low pH of 8.5-9 will facilitate the reinforced steel bars to corrode as displayed in **Fig. 3** resulting in the following reactions where the formed corrosion products is 2-4 times greater in volume than the original.

$$2Fe + O_2 \rightarrow 2FeO$$

$$FeO + H_2CO_3 \rightarrow FeCO_3 + H_2O$$

$$4FeCO_3 + 10H_2O + O_2 \rightarrow 4Fe(OH)_3 + 4\ H_2CO_3$$

Once corrosion sets in, the crack generated will pave the way for water and oxygen as well as carbon-di-oxide to permeate and react with $Ca(OH)_2$ which is a main factor in passivating the steel surface. Carbonation corrosion does not work in all the cases where the enough thickness of the concrete cover if present hinders the penetration of water and oxygen.

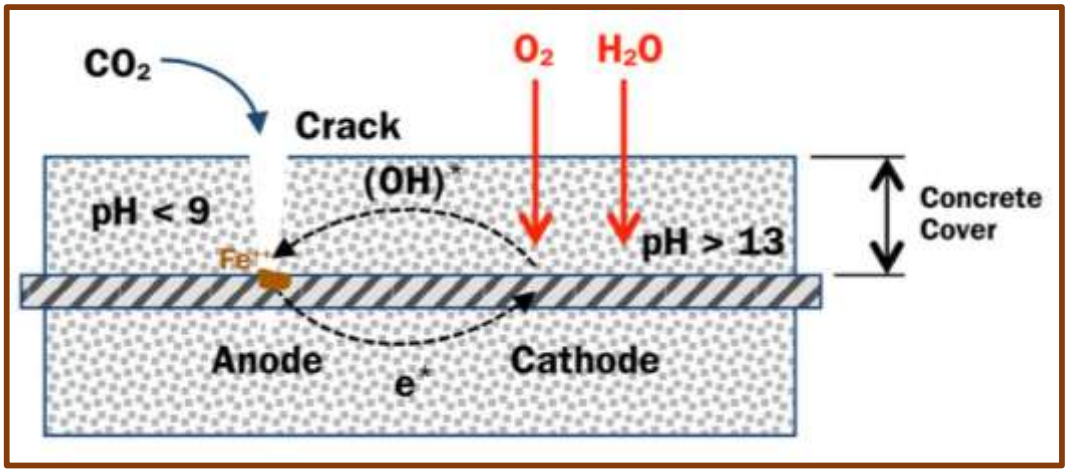

Fig. 3 Schematic illustration of carbonation corrosion

7.1.3.2 Chloride corrosion

One of the most common triggering factor of rebar corrosion is the chloride ions which has the capability of originating near the steel surface initially followed by the breakdown of passive film[16]. These chlorides can enter either from the contaminated concrete mix which could be obviously from sea water, ground water, salt spray or deicing salts in fresh state or in hardened state from sorroundings. Diffusion of these chloride ions into the concrete starts when there is a decline in pH level ie., 13 to 9 as reported by most of the researchers[17-19]. **Montemor *et al.*,**[20] reported that the destruction of passive layer starts due to the replacement of O^{2-} ions from the passive layer by Cl^- ions as shown in **Fig. 4**. This results in the lowering of interfacial surface tension thereby inducing cracks and flaws as documented by Hoar in 1967.

Insoluble calcium chloroaluminates and calcium chloroferrites in which the chloride is bonded in non-active form[21] results due to the reaction occurring between chlorides and calcium aluminates (C_3A) and calcium aluminoferrite (C_4AF) of concrete. However some active soluble chlorides always remain in equilibrium in the aqueous phase of concrete whose concentration level decides the risks of corrosion. Thus the amount of chloride in the concrete and the amount of free chloride in the aqueous phase (which is partly a function of cement content and also of the cement type) will influence the extent of corrosion. In general, chloride

ions are not consumed in the process but catalyses the corrosion reaction by depassivating the protective layer Fe_2O_3 thereby initiating quick degradation of structures[22].

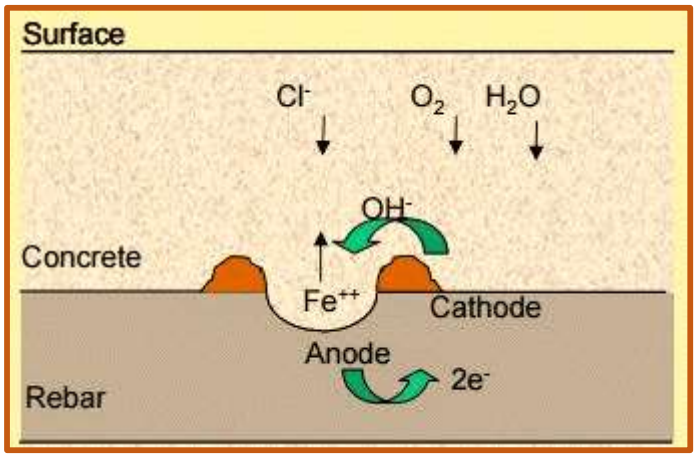

Fig. 4 Schematic illustration of chloride induced corrosion

7.1.4 Sequence of degradation

The reinforced concrete suffers corrosion via corrosion initiation and propagation whose step wise degradation can be clearly dealt with the help of the illustration shown in **Fig. 5**.

(i) During the initiation phase, depassivating substances like CO_2 (or) Cl^- ingress through the concrete coverage favouring depassivation of the layer. The time taken to break the passive layer is denoted as time of corrosion initiation phase shown as 1 in the below illustration

(ii) The spot 2 indicates the propagation phase leading to the iron dissolution whose rate is controlled by number of factors like availability of oxygen, moisture and temperature.

(iii) Remarkably 6 to 8 fold increase in corrosion product will be generated than the original volume of steel consumed leading to significant spalling and cracking of the concrete cover.

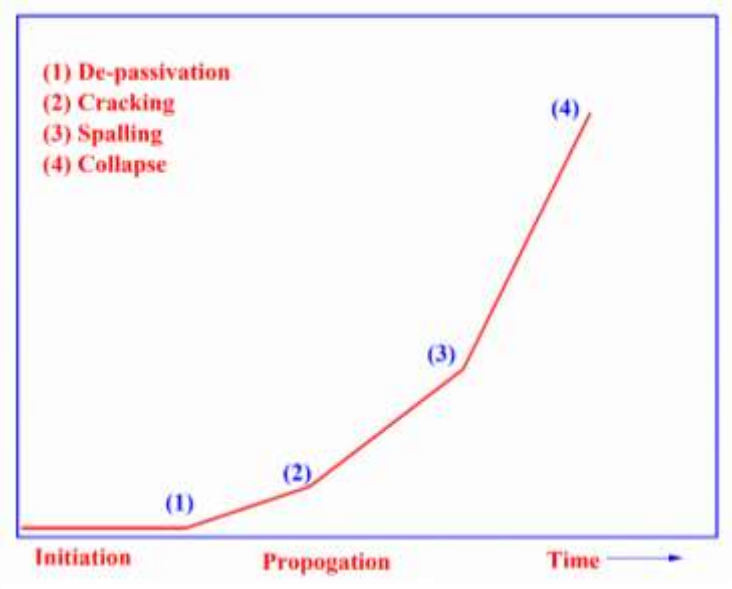

Fig. 5 Sequence of degradation in rebar corrosion

7.1.5 Review of literature

To start with, review made on various aspects of rebar corrosion are summarised below,

Hongfang Sun *et al.,* employed carbon fibre reinforced polymer (CFRP) as an impressed current anode and studied its corrosion process in 3% sodium chloride medium. As a result a failure mechanism was noticed due to the corrosion of epoxy matrix which led to the breakage of C-N bonds leading to a depolymerisation reaction[23].

The corrosion inhibition of reinforced mortar in presence of both empty and calcium containing vesicles based on polyethylene oxide-b-polystyrene (PEO_{113}-b-PS_{780}) was documented by **Hu *et al.,***. Results revealed that calcium containing vesicles rendered increased resistance towards corrosion. Initial formation of barrier as well as later release of calcium from calcium containing vesicles led to the modification of steel surface[24].

Four commercially available concrete coatings comprising of three elastomeric coatings and a cementious mortar modified with polymer were studied by **Brenna *et al.,*** under chloride induced medium. Analysis showed that the coating based on cement provided a good physical barrier for the penetration of chloride ions irrespective of polymer content present. In addition, coatings rendered reduced water movement which is prime factor in inducing corrosion[25].

Hola *et al.,* analysed the role of polymer sulphur composites in protection of reinforced corrosion. After analysing, the optimum compositions were chosen to carry out the experimental research in a detailed manner[26].

Mariusz Ksiazek predicted the results obtained by subjecting polymer coating to steel reinforced bars in simulating pore solution under tensile stress. Parameters obtained from potentiodynamic polarisation techniques exhibited decreased corrosion rate in orders of magnitude for coated areas. A non-coated area also experienced decreased corrosion rate when immersed in model pore solution[27].

Diamanti *et al.,* studied the improved durability of reinforced concrete in presence of cement and organic based coatings under chloride induced medium. They were expected to act as physical barrier thereby retarding the penetration of ions, gases and water responsible for corrosion. Tests carried out on coated specimens gave the relevant information about the chloride penetration, decreased water content as well as life of concrete structures[28].

Mantas Atutis *et al.,* summarised the cracking growth, deflection and flexural stiffness obtained from the experimental investigation of composite material like basalt fiber reinforced polymers (BFRP). As a motto of expanding its applications in industry, research based on BFRP was also explored[29].

Marianne Inman *et al.,* utilised basalt fibre reinforced polymer (BFRP) rebar against conventional steel rebar to compare its mechanical and environmental performance. Material testing and life cycle assessment showed that BFRP reinforced fibres were found to be stronger and lighter when compared with steel[30].

Stefano De Santis *et al.,* compared steel reinforced polymers (SRP) with already known carbon and glass fibre reinforced polymers where the former exhibited better tensile bond strength and good load bearing capacity. Research carried out has shown that usage of SRPs is a cost effective method to renovate the structures which could be designed similarly as done for fibre reinforced polymers (FRP)[31].

An investigation based on PVC embedded reinforced concrete under load was reported by **Amr Abdel Havez *et al.,*.** The embedded wall projected more ductility and superior performance in comparison with control wall specimens. An analytical model was performed where the experimental and calculated peak loads were in good agreement[32].

Aramid fiber reinforced polymer (AFRP) confined concrete under high strain rate was investigated by **Hui Yang *et al.,*.** Experimental results revealed that the properties such as ultimate strain, energy absorption and dynamic strength which were sensitive to strain rate were

significantly improved by AFRP. Mechanism associated with strengthening and toughening of AFRPs were also carried out[33].

Krishneel *et al.,* conducted a laboratory controlled experiment to access the rebar corrosion in presence of chlorides which is a well-known corrosion process in presence of other cations like sodium chloride, potassium chloride and magnesium chloride. Investigation of concrete-steel interfacial corrosion was studied by adopting galvanostatic pulse technique whose experimental results were fitted with modified Randles circuit. Comparison made among the cations, revealed the corrosive nature of sodium to be predominant[34].

Sawpan *et al.,* evaluated the durability of pultruded glass fibre reinforced polymer (GFRP) composite rebar in alkaline medium with various time intervals like 0, 1, 2, 3, 4, 6, 14 and 24 months at a temperature range of 60 °C. It was observed that 91.5% of glass transition temperature and short beam shear strength was retained when the ageing process started from 0 to 24 months. Scanning electron microscopy and energy dispersive spectroscopy supported the degradation of GFRP whereas it was unable to predict from FT-IR[35].

Fazayel *et al.,* investigated the role of polycarboxylate derivatives containing different functional groups and comonomers in controlling the steel corrosion by adoptiong impedance and polarisation techniques. The studies carried out in the presence of alkaline medium showed the corrosion retardation in the order of poly methacrylate-co acrylamide > poly methacrylate-*co*-2-acrylamido-2 methylpropane sulfonic acid > poly methacrylate-*co*-hydroxyethylmetha crylate. The inhibition action of these reported polymers were supposed to form a barrier on the surface as evident from SEM, EDS and AFM analysis[36].

Kodur *et al.,* documented a numerical method to access the extent of fibre reinforced polymer (FRP) concrete in presence of fire. This model evaluated the influence of temperature on steel, concrete, FRP and bond existing between concrete and FRP. Fire tests were fixed as standards to compare the response of FRPs. Investigations based on case studies revealed that, besides conventional RC slabs, FRP yielded lower fire resistance[37].

Sharkawi *et al.,* selected long natural yarns comprising of short flax and jute fibres to reinforce the polyester bars (NYRP) by means of infusion technique where the volume fraction ratios of fibres were modified. Microscopic images supported a good distribution across NYRP fibres. Though the NYRP fibres were associated with good tensile strength, stiffness and ductility, it resulted in failure when reinforced with concrete slabs[38].

Al-Majidi *et al.,* reported the corrosion protection rendered by polyvinyl alcohol fibre reinforced geopolymer concrete. Induced current technique was used to study the accelerated

corrosion test for a duration of 90 days. The results revealed better structural performance where the accelerated corrosion followed later[39].

Based on the above review, a possible strategy can be decided in order to minimise the rebar corrosion. Besides inorganic inhibitors which were banned due to its carcinogenic nature[40] and organic inhibitors[41] such as N, N'-dimethyl aminoethanol, diethanolamine, amines, alkanolamines and carboxylates whose synthetic strategy and toxic nature has limited its usage, polymers has gained remarkable attention due to its multiple adsorption sites, facile synthesis, low cost and capability of adsorbing larger surface[42]. In order to support the fact that, limited research work has been carried out on polymers like poly (vinyl pyrolidone), poly ethylamine, polyaniline, polyethylene glycol, polysiloxane, poly vinyl alcohol, polyethylene glycol methyl ether in reinforced concrete corrosion, this present work has been undertaken to explore the response of aliphatic and aromatic polyesters in simulated concrete pore solution by adopting electrochemical techniques.

7.2 EXPERIMENTAL METHODS

7.2.1 Inhibitor

The synthesised inhibitors PGAZ and PGSE containing aliphatic moieties as well as MPOB and MPOU possessing both aliphatic and aromatic moieties (shown in chapter II) were subjected to evaluate its support in metal (steel) protection under alkaline electrolytic medium. The following are the structure of inhibitors involved in the present discussion.

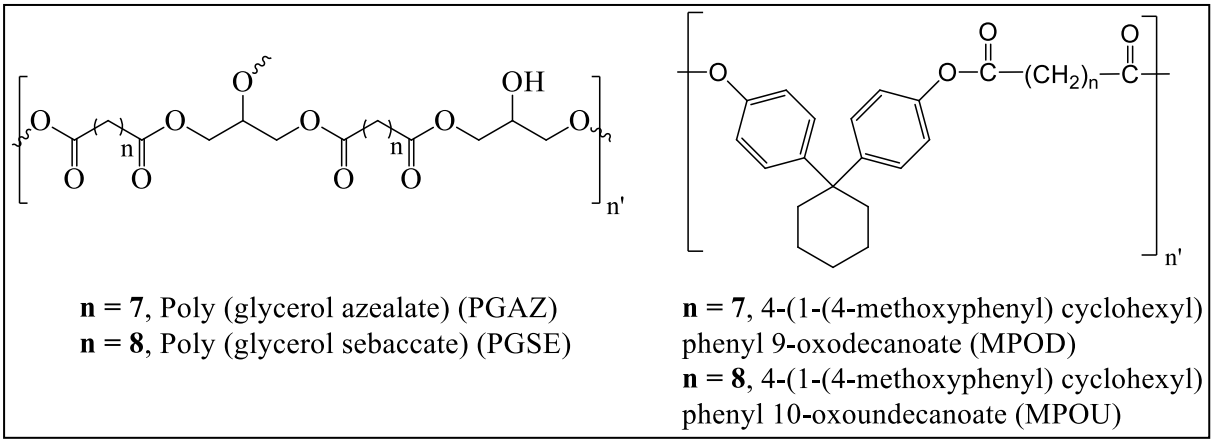

n = **7**, Poly (glycerol azealate) (PGAZ)
n = **8**, Poly (glycerol sebaccate) (PGSE)

n = **7**, 4-(1-(4-methoxyphenyl) cyclohexyl) phenyl 9-oxodecanoate (MPOD)
n = **8**, 4-(1-(4-methoxyphenyl) cyclohexyl) phenyl 10-oxoundecanoate (MPOU)

7.2.2 Preparation of the electrolyte

The simulated concrete pore solution (SCP) used as electrolytic medium in the present discussion was made by mixing 0.5 M $Ca(OH)_2$, 0.5 M KOH and 0.1 M NaOH of required quantity whose pH was maintained around 13 followed by the addition of 0.5 M NaCl solution gradually decreasing the pH to simulate a corrosive environment[43].

7.2.3 Moulding of specimens

The specimens were made by cutting cylindrical steel rebar grade 60 [ASTM A615] of required length with an exposed area of 1 cm^2. The surface finishing procedure was done by following the standard practice of using various grades of silicon carbide sheets, degreasing with acetone until mirror finish polish was ensured.

7.2.4 Electrochemical measurements

The popularity of applying electrochemical methods for reinforced concrete has increased remarkably in recent years. As a continuation, to explore the corrosion behaviour of preferred rebar specimens in simulated concrete pore solution, an electrochemical work station with a three electrode assembly was set up with a platinum foil as counter electrode and calomel electrode as standard reference electrode along with a steel working electrode of 1 cm^2 exposed area. The tests were performed at room temperature with a net content of 100 ml electrolyte whose results were deduced from computer assisted IVIUM compactstat software.

a) Electrochemical impedance spectroscopy (EIS)

A conventional three electrode system was used to carry out the electrochemical impedance analysis. The simulated concrete pore solution (SCP) contaminated with Cl^- ions having the ratio of 0.5 M $Ca(OH)_2$, 0.5 M KOH, 0.1 M NaOH and 0.5 M NaCl was used as electrolyte (Blank) throughout the studies. Blank solution without Cl^- contamination was used for comparison purpose as the chlorides are the major factor in initiating corrosion in reinforced concretes. The corrosion inhibition and protecting nature of inhibitors dispersed in blank medium was measured after attaining open circuit potential with a 10 mV amplitude signal at applied frequency range of 10 KHz to 0.01Hz. The electrochemical parameters obtained were applied in the below expression to calculate its inhibition efficiency (IE)[44] and surface coverage (Θ)[45].

$$\text{Inhibition efficiency (\%)} = \frac{R_{ct(inh)} - R_{ct(blank)}}{R_{ct(inh)}} X100 \quad (1)$$

$$\text{Surface coverage } (\Theta) = \frac{\text{Inhibtion effeciency(\%)}}{100} \quad (2)$$

where $R_{ct(inh)}$ and $R_{ct(blank)}$ represents charge transfer resistance of inhibited and uninhibited medium and Θ represents surface coverage.

b) Potentiodynamic polarisation studies

The electrochemical behaviour of concrete was studied by potentiodynamic polarisation technique using the similar set up. The experiments were programmed to polarise the specimen at a potential of ± 200 mV vs OCP in both the directions (ie.) cathodic and anodic regions with a scan rate of 1mV/sec. From the extrapolation of Tafel slopes, the current corresponding to each potential was recorded with the aid of computer assisted IVIUM compactstat software. From the evaluated corrosion parameters like I_{corr}, E_{corr}, b_a and b_c the inhibition efficiency was calculated using the below expression[46],

$$\text{Inhibition efficiency (\%)} = \frac{I_{corr(blank)} - I_{corr(inh)}}{I_{corr(blank)}} X100 \quad (3)$$

where $I_{corr(blank)}$ & $I_{corr(inh)}$ represents corrosion current in the absence and presence of inhibitor.

7.2.5 Study on morphology-Scanning electron microscopy analysis (SEM).

Scanning electron microscopic images were recorded using ZIESS SEM analyser for the specimens immersed in non-chlorinated and chlorinated medium along with optimum concentration of the inhibitors PGAZ and MPOD to inspect the surface morphological texture.

7.3 RESULTS AND DISCUSSION

7.3.1 Electrochemical impedance spectroscopy (EIS)

EIS study of rebar in absence and presence of selected concentrations (10, 100, 1000 ppm) of polyesters were recorded in the form of Nyquist plot which shows the relationship between electrical resistance and applied frequency[47]. Plots corresponding to impedance measurements are displayed in **Figs. 7.1-7.5** and the data are listed in **Table 7.1** and **Table 7.2**. On examining **Fig. 7.1** and data from **Table 7.1**, the decreased R_{ct} values (112.08 ohm cm^2) of simulated concrete pore solution (SCP) with chloride ion compared to non-chlorinated medium (213.24 ohm cm^2) clearly demonstrated that the rebar has suffered severe corrosion under chloride induced medium. The obtained EIS data were fitted into two time constant equivalent circuits as shown below in **Fig. 6** in order to model the rebar-solution interface in the absence and presence of inhibitors.

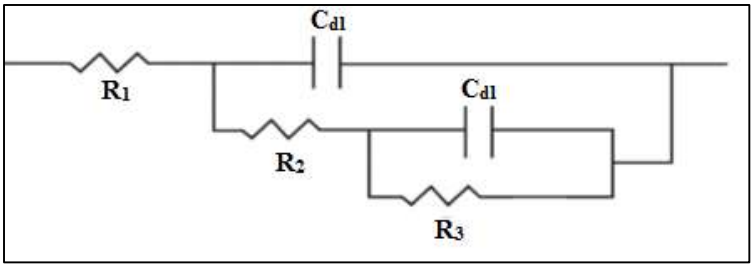

Fig. 6 Proposed equivalent circuit

On addition of inhibitors, the increase in R_{ct} values suggested that the amount of inhibitor adsorbed on the reinforced steel surface increased[48] favouring the formation of diffused layer[49] consequently resulting in decrease of active sites where dissolution of iron is facilitated. This surface barrier effectively prevents the ingress of Cl^- ion and oxygen concentration close to the metal surface thereby inhibiting corrosion. In the present discussion, the highest inhibition efficiency of 75.28% observed for MPOU was associated with decreased C_{dl}[50] and increased R_{ct} rendering slow corrosion system[51] which is due to the aromatic cloud of benzene ring[52] as shown in **Table 7.2**. The imbalance of charges due to the existence of ions on the solution side and electrons on the metal side causes deviation from ideal capacitor behaviour[53]. Moreover the deviation from the expected semicircles of Nyquist plot to a straight line pattern suggested diffusion controlled mechanism rather kinetically controlled one[44] which created a blanketing effect rendering passive state[54].

7.3.2 Potentiodynamic polarisation technique

Reinforced steel never remains passive in alkaline pore solution where the chloride ions tends to be more reactive to render corrosion. **Fig. 7.6** depicts the polarisation curves of the pore solution and simulated pore solution. In the absence of chloride ions, the steel remained passive whereas the ingression of chloride ions decreased the potential as shown[55]. Chloride induced severe attack was confirmed from the increased I_{corr} values observed for simulated concrete pore solution (SCP) with chloride ions[56] as displayed in **Table 7.3**. **Figs. 7.7-7.10** exhibited the polarisation curves of rebar in presence of selected concentrations of the inhibitor. It is evident from the polarisation parameters listed in **Table 7.4**, that the inhibition efficiency is more pronounced by increasing the polymeric additives suggesting the formation of barrier on the steel surface thereby retarding the corrosion[51]. Higher rate of metal protection rendered by the inhibitors MPOU and MPOD was evidenced from decreased corrosion current density (I_{corr}) compared to moderate efficiency of PGAZ and PGSE. Successive decrease in I_{corr} values suggested continuous passivation avoiding permeation of Cl^- ions[57]. Close observation of E_{corr} values revealed shift towards more negative direction as well as the changes experienced in E_{corr} values was about 206.6 mV representing the cathodic inhibition by reducing the hydroxide evolution[58] which is in agreement with $E_{corr} > 85$ mV[59].

7.3.3 Inhibition efficiency, surface coverage and adsorption isotherm

The inhibition efficiency and surface coverage of the polymeric inhibitors in alkaline pore solution contaminated with chloride ions (blank) were calculated from the polarization

data as shown in **Table 7.4**. The variation of inhibition efficiency as a function of inhibitor concentration was also observed. The adsorption isotherm was studied by fitting the experimental data as shown in the plot of C/Θ vs. C (**Fig. 7.11**). The efficiency of polymer moiety was moderate to good which mainly depended on their adsorption ability on the rebar surface. Hence, the investigation of the relation between corrosion inhibition and adsorption is of great importance. Analysis proved that, the adsorption of polymer at the metal-solution interface took place through the replacement of water molecules by added polymers through the inherent bonding and lone pair of electrons. Experimental results were best fitted with Langmuir adsorption isotherm model with R^2 near to unity[60] representing monolayer adsorption. It should also be noted that the orientation of aromatic rings, side chains and steric effects by bulky groups are not only always participated or adsorbed parallel to the surface of metal, sometimes it can be of networking on the surface, thereby increasing hydrophobicity. It is also agreed from the results that while increasing the concentration of polymer, surface coverage on rebar also increased[56].

7.3.4 Study on morphology-Scanning electron microscopy analysis (SEM).

The morphological images displayed in **Fig. 7.12(a)** ensured the absence of chloride attack retaining its passive surface to an extent, whereas **Fig. 7.12(b)** clearly indicated that the rough and cracked surface[61] was due to the ingress of chloride ions. But better surface coverage performance[62] observed in **Figs. 7.12(c,d)** was due to the presence of inhibitors PGAZ and MPOD which has displaced the chloride ions from the surface and blocked the active sites rendering minimised depassivation which is an intermediate between passivation and corrosion state[63] representing that the passive film was not completely destroyed favouring smoother surface in case of MPOD than PGAZ.

7.3.5 Mechanism

Metal dissolution in rebar might be chemical or electrochemical which is mostly facilitated by the intrusion of chloride and carbonates[64,65]. In such a condition the efficiency of the added polymers mainly depends on their adsorption ability on the rebar surface. General observations revealed that the inhibitors bond to the metals by adsorption either physically or chemically based on which it can be categorised into adsorptive or layer forming type. Most of the inhibitors play dual role of blocking (adsorbed) both cathodic and anodic reactions and forming passive layer of iron oxide reducing the mobility between the steel and concrete interface thereby dropping the corrosion rate[66]. The main reason leading to the acceleration of corrosion of steel bar in concrete is the wetting-drying cycles that can increase the corrosion

potential difference between anode and cathode of steel bar which is the actual driving force resulting in decreased concrete resistance[3]. Also the corrosion reaction which is an oxidation reaction leading to break down of passive film[67] is mainly facilitated by the electrolyte that can carry ions which is alkaline pore solution of concrete in the present discussion.

Detailed insight of mechanism showed that the steel remains as cathode in reinforced concrete until depassivation occurs. As it begins to occur either by reduction in pH or local break down, part of the steel behaves as cathode and part behaves as anode initiating corrosion. Anodic reaction is facilitated by the movement of Fe to Fe^{2+} with liberation of electrons making more negative potential on a part of steel and enhances the current flow in the pore solution. The electrons generated moves towards the cathode where they get adsorbed by the constituents of the electrolyte and combine with water and oxygen to form hydroxyl ions (OH^-)[12]

$$Fe \longrightarrow Fe^{2+} + 2e^-$$

$$O_2 + 1/2\ H_2O + 2e^- \longrightarrow 2OH^-$$

In order to minimize the cathodic and anodic reaction, the added inhibitor will function according to any one of the following possibilities[56].

- Formation of quaternary salt by binding inhibitor molecules with chloride ions leading to the formation of protective layer anchored on adsorption sites of the rebar surface
- Adsorption of gel like complexes formed between the inhibitor and Cl^- ion present in the simulated pore solution on the metal surface.
- Gel impregnation of rebar surface takes place reducing the penetration of Cl^-, O_2 and H_2O.

The polymers added inhibit corrosion of steel by means of displacing Cl^- ions present on the rebar surface and preferentially adsorb on the metal surface by its lone pair of electrons and π electron density of aromatic anchoring sites in case of cardo polyesters (MPOD and MPOU) followed by interaction of lone pair electrons of aliphatic moieties (PGAZ and PGSE) and protecting the metal surface from the attack of aggressive Cl^- ions as shown in **Fig. 7.13**. This is also evident from the significant reduction in corrosion current (I_{corr}) and increase in R_{ct} values when the inhibitor enters into the pore solution medium thereby retarding the metal dissolution by suppressing the penetration of Cl^- ions onto the metal surface. The common mechanism assumed is the competitive adsorption of Cl^- and OH^- ions on the passive film. Higher chloride content makes the probability of substituting chloride ions in sufficient number

of adjacent sites initiating the rupture of passive film[55]. Thus the added additives might displace Cl^- ions or form gel like adduct with added polymers in turn reducing the corrosion phenomena.

7.3.6 Evaluation of the inhibitors

Despite evaluation of the inhibition efficiency, the study of structure activity relationship seems to be important. The surface coverage of aliphatic polyesters favoured by the alkyl spacers along with lone pair electrons was sufficiently less in comparison to cardo polyesters where the aromatic rings rich in pi-electron density governed with alkyl moieties predominantly influenced the adsorption to a good extent. The techniques applied to evaluate the rebar corrosion is in good harmony of increased inhibition efficiency due to the following reasons[58].

- The aromatic sites are more voluminous than methyl groups, forming an effective physical barrier that can block (or) delay the chloride arrival to the metal surface. Thus both bulky aromaticity and electronic property of phenyl group contributed better inhibition efficiency in case of MPOD and MPOU.
- On investigating the aliphatic polyesters strange behaviour in inhibition efficiency was noticed due to the absence of aromaticity. At the same instant, a moderate efficiency was favoured by the alkyl spacers and the lone pair electrons of heteroatoms adsorbed on the metal surface.
- Examining the investigated polymers in various aspects, its metal protection capability is framed according to the following order

MPOU > MPOD > PGSE > PGAZ

7.4 CONCLUSIONS

Based on the study of corrosion inhibitive performance of the aliphatic and aromatic polyesters, in simulated and chloride contaminated pore solution (blank),the following conclusions were drawn,

- Polarization studies indicated the formation of a protective film preventing the ingress of aggressive ions towards rebar in alkaline medium.
- Impedance studies also proved the same which was evident from increased charge transfer resistance and inhibition efficiency.
- The adsorption of polyesters on metal surface in mitigating the corrosion was revealed from the SEM images.

- Surface coverage values were best fitted with Langmuir adsorption isotherm suggesting monolayer adsorption.
- Investigated polymers with similar back bone differed in inhibiting nature due to the variation of aliphatic and aromatic moieties.
- The following order of inhibition efficiency was found from the present discussion

MPOU > MPOD > PGSE > PGAZ

7.5 REFERENCES

1. A. Brenna, S. Beretta, F. Bolzoni, M. Pedeferri, M. Ormellese, Constr. Build. Mater., **137** (2017) 76–84.
2. Y. Tian, C. Dong, X. Cheng, Y. Wan, G. Wang, K. Xiao, X. Li, Constr. Build. Mater., **151** (2017) 607–614.
3. A.H. Essam, A. Zubaidy, A.A. Tamimi, Int. J. Electrochem. Sci., 7 (2012) 6472-6488.
4. S. Muthulingam, B.N. Rao, Corros. Sci., **93** (2015) 267–282.
5. H. Gurdian, E. García-Alcocel, F. Baeza-Brotons, P. Garces, E. Zornoza, Mater., **7** (2014) 3176-3197.
6. J.D. Moreno, M. Bonilla, J.M. Adam, M.V. Borrachero, L. Soriano, Constr. Build. Mater., **100** (2015) 11–21.
7. H. Verbruggen, H. Terryn, I.D. Graeve, Constr. Build. Mater., **124** (2016) 887–896.
8. X. Wang, J. Wang, X. Yue, Int. J. Electrochem. Sci., **9** (2014) 6558-6571.
9. H. Bruno, V.L. Hostis, F. Miserque, H. Idrissi, Electrochim. Acta., **51** (2005) 172-180.
10. J.M. Deus, B. Diaz, L. Freire, X.R. Novoa, Electrochim. Acta., **131** (2014) 106–115.
11. O. Poupard, V.L. Hostis, S. Catinaud, I. Petre-Lazar, Cem. Concr. Res., **36(3)** (2006) 504-520.
12. F. Shaheen, B. Pradhan, Constr. Build. Mater., **101** (2015) 99–112.
13. P.D. Cady, R.E. Weyers, Cem. Concr. Aggt., **5(2)** (1983) 81-87.
14. R. Francois, G. Arliguie, Mag. Concr. Res., **51(2)** (1999) 143–150.
15. O.B Isgor, A.G Razaqpur, Cem. Concr. Compos., **26** (2004) 57-73.
16. M. Moreno, W. Morrism, M.G. Alvarez, G.S. Duffo, Corros. Sci., **42(11)** (2004) 2681-2699.
17. C. Alonso, M. Andrade, X.R. Izquierdo, M.C. Novoa, Perez, Corros. Sci., **40** (1998) 1379-1389.
18. D. Trejo, P.J. Monteiro, Cem. Concr. Res., **35** (2005) 562–571.
19. T. Maheswaran, J.G. Sanjayan, Mag. Concr. Res., **56(6)** (2004) 359–366.
20. M.F. Montemor, A.M.P Simoes, M.G.S. Ferreira, Cem. Concr. Compos., **25** (2003) 491-502.
21. F.K. Matlob, A.M.A Amir, JKU., **6** (2008) 121-139.
22. H.W. Song, V. Saraswathy, Int. J. Electrochem. Sci., **2** (2007) 1-28.
23. H. Sun, L. Wei, M. Zhu, N. Han, Z. Ji-Hua, F. Xing, Constr. Build. Mater., **112** (2016) 538-546.
24. J. Hu, D.A. Koleva, P. Petrov, K.V. Breugel, Corros. Sci., **65** (2012) 414-430.

25. A. Brenna, F. Bolzoni, S. Beretta, M. Ormellese, Constr. Build. Mater., **48** (2013) 734-744.
26. J. Hola, M. Ksiazek, Arch. Civ. Mech. Eng., **9(1)** (2009) 47-59
27. Mariusz Ksiazek, Compos. Part B: Eng., **42(5)** (2011) 1084-1089.
28. M.V. Diamanti, A. Brenna, F. Bolzoni, M. Berra, T. Pastore, M. Ormellese, Constr. Build. Mater., **49** (2013) 720-728.
29. M. Atutis , J. Valivonis, E. Atutis, Compos. Struct., **183** (2018) 114-123.
30. M. Inman, E.R. Thorhallsson, K. Azrague, Energy Procedia., **111** (2017) 31-40.
31. S.D. Santis , G. Felice, A. Napoli, R. Realfonzo, Compos. Part B: Eng., **104** (2016) 87-110.
32. A.A. Havez , N. Wahab, A. Al-Mayah, K.A. Soudki, Struct., **5** (2016) 67-75.
33. H. Yang, H. Song, S. Zhang, Constr. Build. Mater., **95** (2015) 143–151.
34. K.K. Sharma, R.N. Deo, A. Kumar, K. Mamun, Constr. Build. Mater., **165** (2018) 533-540.
35. M.A. Sawpan, A.A. Mamun, P.G. Holdsworth, Mater. Des., **57** (2014) 616-624.
36. A.S. Fazayel, M. Khorasani, A.A. Sarabi, Appl. Surf. Sci., **441** (2018) 895-913.
37. V.K.R. Kodur, P.P. Bhatt, Compos. Struct., **187** (2018) 226-240.
38. A.M. Sharkawi, A.M. Mehriz, E.A. Showaib, A. Hassanin, Constr. Build. Mater., **158** (2018) 359-368.
39. M.H. Al-Majidi, A.P. Lampropoulos, A.B. Cundy, O.T. Tsioulou, S. Al-Rekabi, Constr. Build. Mater., **164** (2018) 603-619.
40. S. Jiang, L. Hua Jiang, Z. Yin Wanga, M. Jin, S. Bai, S. Song, X. Yan, Constr. Build. Mater., **150** (2017) 238–247.
41. H. Ryu, J. K. Singh, H. Seung, M.A. Ismail, W. Park, Constr. Build. Mater., **133** (2017) 387–396.
42. A.F.S. Abdul Rahiman, S. Sethumanickam, Arab. J. Chem., **10** (2017) 3358-3366.
43. J. Jiang, D. Wang, H. Chu, H. Ma, Y. Liu, Y. Gao, J. Shi, W. Sun, Mater., **10** (2017) 1-14.
44. G. Madhusudhana, R. Jaya Santhi, IJSR. NET., **4** (2015) 1645-1650.
45. A. Jamal, M. Nasser, M. Anwar Sathiq, Arab. J. Chem., **9** (2016) 691-698.
46. G. Karthik, M. Sundaravadivelu, Egypt. J. Pet., **25** (2016) 183-191.
47. V. Trianaa, J.L. Marriagaa, J.O. Florez, Mat. Res., **16** (2013) 1457-1464.
48. N. Soltani, N. Tavakkoli, M. Ghasemi, Int. J. Electrochem. Sci., **11** (2016) 8827-8847.

49. H.S. Ryu, J.K. Singh, H.M. Yang, H.S. Lee, M.A. Ismail, Constr. Build. Mater., **114** (2016) 223–231.
50. A. Pal, S. Dey, D. Sukul, Res. Chem. Intermed., **42** (2016) 4531-4549.
51. A.S. Fouda, G.Y. Elewady, K. Shalabi, H.K. Abd El-Aziz, RSC Adv., **5** (2015) 36957-36968.
52. A.A. Farag, A.S. Ismail, M.A. Migahed, J. Mol. Liq., **211** (2015) 915-923.
53. K. Cellat, F. Tezcan, B. Beyhan, G. Kardas, H. Paksoy, Constr. Build. Mater., **143** (2017) 490-500.
54. Y. Guo, X.P. Wang, Y.F. Zhu, J. Zhang, Y.B. Gao, Z.Y. Yang, R.G. Du, C.J. Lin, Int. J. Electrochem. Sci., **8** (2013) 12769-12779.
55. M. Cabrini, F. Fontana, S. Lorenzi, T. Pastore, S. Pellegrini, J. Chem., **2015** (2015) 1-10.
56. B. Bhuvaneshwari, A. Selvaraj, N.R. Iyer, L. Ravikumar, Mater. Corros., **66** (2015) 387-395.
57. A.U. Malik, I. Andijani, F. Al-Moaili, G. Ozair, Cem. Concr. Compos., **26** (2004) 235-242.
58. J.Z. Liu, D. Zhao, J.S. Cai, L. Shi, J.P. Liu, Int. J. Electrochem. Sci., **11** (2016) 1135-1151.
59. T.K. Chaitra, K.N. Mohana, D.M. Gurudatt, H.C. Tandon, J. Taiwan Inst. Chem. Eng., **67** (2016) 521-531.
60. X. Su, C. Lai, L. Peng, H. Zhu, L. Zhou, L. Zhang, X. Liu, W. Zhang, Int. J. Electrochem. Sci., **11** (2016) 4828-4839.
61. A. Cesen, T. Kosec, A. Legat, V.B. Bosiljkov, Mater. Tehnol., **48** (2014) 51-57.
62. A.M. Masmoudi, J. Bouaziz, Adv. Mater. Sci. Eng., **2016** (2016) 1-6.
63. C. Sun, S. Liu, J. Niu, W. Xu, Int. J. Electrochem. Sci., **10** (2015) 5309-5326.
64. S.K. Verma, S.S. Bhadauria, S. Akhtar, Scientific World J., **2014** (2014) 1-9.
65. G. S. Hurtado, M.A.B. Zamora, R.G. Martinez, L.D. Lopez, F. Zapata, P. Zambrano, C.G. Tiburcio, F.A. Calderon, Int. J. Electrochem. Sci., **11** (2016) 4850-4864.
66. C.G. Berrocal, K. Lundgren, I. Lofgren, Cem. Concr. Res., **80** (2016) 69-85.
67. N.P.D. Alcantara, F.M.D. Silva, M.T. Guimaraes, M.D. Pereira, Sens., **16** (2016) 1-18.

Table 7.1 AC-impedance parameters for pore solution in the absence and presence of chloride ions

Electrolyte medium (M)	R_{ct} (ohm cm^2)	C_{dl} (µF/cm^2)
Pore solution without Cl^-	213.24	138.21
Pore solution with Cl^-	112.08	192.4

Table 7.2 AC-impedance parameters for rebar corrosion for selected concentrations of the polyesters

Name of the inhibitor	Conc. (ppm)	R_{ct} (Ohm cm^2)	C_{dl} (µF/cm^2)	Inhibition efficiency (%)
Pore solution with Cl^-	-	112.08	192.4	-
PGAZ	10	201.25	65.05	44.30
	100	232.08	49.32	51.71
	1000	297.34	42.89	62.31
PGSE	10	209.59	51.85	41.11
	100	245.88	43.21	49.80
	1000	311.27	40.08	60.09
MPOD	10	265.3	49.35	57.75
	100	345.81	33.33	67.58
	1000	451.02	30.19	75.14
MPOU	10	252.57	42.94	51.13
	100	343.34	24.44	64.05
	1000	491.46	17.53	75.28

Table 7.3 Polarization parameters for pore solution with and without chlorine

Electrolyte medium (M)	b_a (mV/dec)	b_c (mV/dec)	$-E_{corr}$ (mV) vs SCE)	I_{corr} ($\mu A/cm^2$)
Pore solution without Cl^-	142	68	659.2	228.87
Pore solution with Cl^-	183	52	563.5	489.64

Table 7.4 Polarization parameters for rebar corrosion for selected concentrations of the polyesters

Name of the inhibitor	Conc. (ppm)	Tafel slopes (mV/dec)		$-E_{corr}$ (mV) vs SCE)	I_{corr} ($\mu A/cm^2$)	Inhibition Efficiency (%)	Degree of surface coverage (Θ)
		b_a	b_c				
Pore solution with Cl^-	-	183	52	563.5	489.64	-	-
PGAZ	10	137	91	696.1	319.20	34.81	0.3481
	100	157	82	698.4	263.23	46.24	0.4624
	1000	136	99	685	244.43	50.08	0.5008
PGSE	10	166	70	727.9	303.82	37.95	0.3795
	100	127	96	770.1	289.67	40.84	0.4084
	1000	114	76	748.5	221.71	54.72	0.5472
MPOD	10	145	93	591.8	302.79	38.16	0.3816
	100	141	99	601.4	217.01	55.68	0.5568
	1000	156	82	611.5	176.22	64.01	0.6401
MPOU	10	117	84	610.6	284.24	41.95	0.4195
	100	144	88	671.1	214.90	56.11	0.5611
	1000	139	99	713.3	158.20	67.69	0.6769

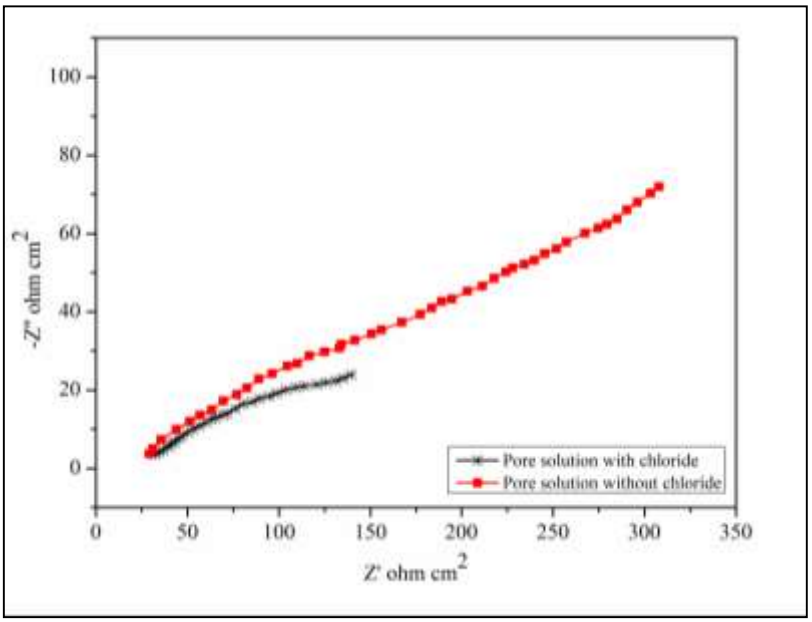

Fig. 7.1 Nyquist plots for pore solution in the absence and presence of chloride ion

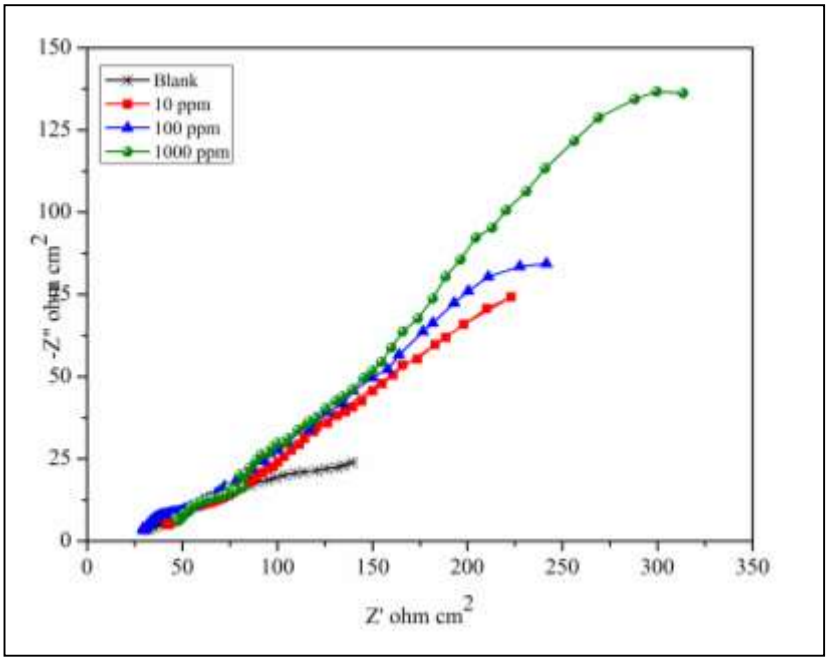

Fig. 7.2 Nyquist plot for selected concentrations of PGAZ in simulated concrete pore solution

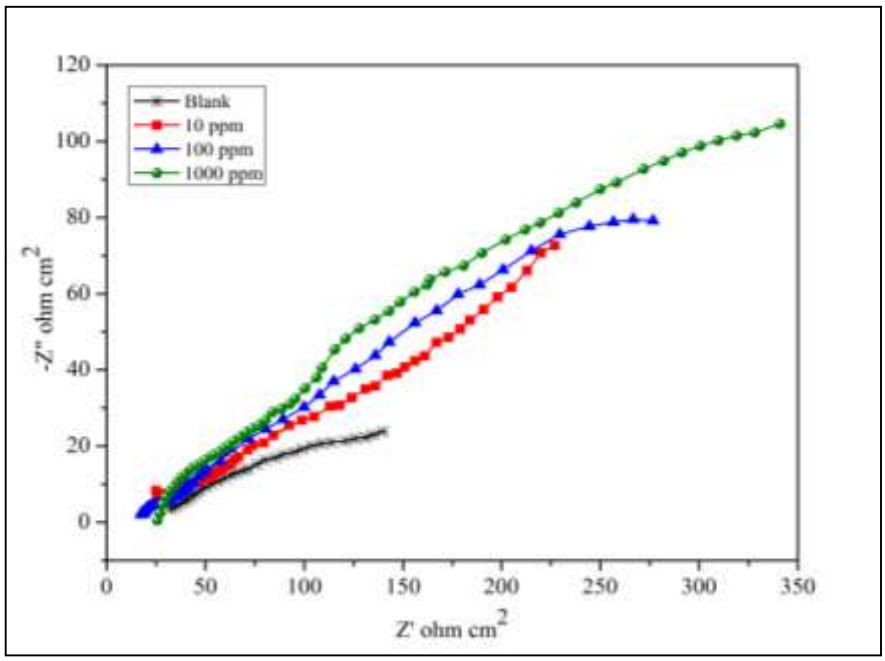

Fig. 7.3 Nyquist plot for selected concentrations of PGSE in simulated concrete pore solution

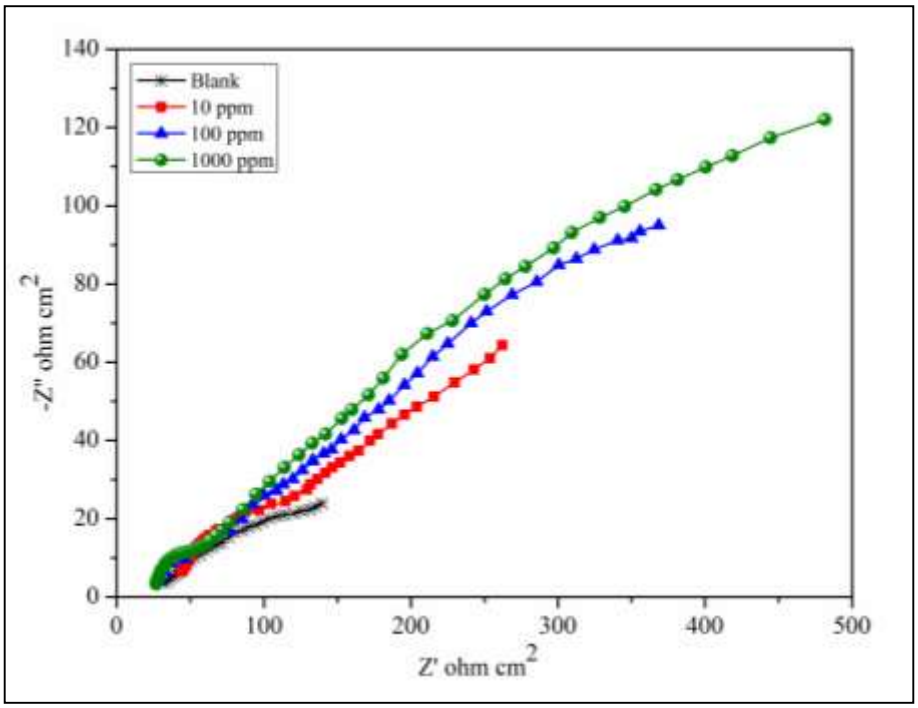

Fig. 7.4 Nyquist plot for selected concentrations of MPOD in simulated concrete pore solution

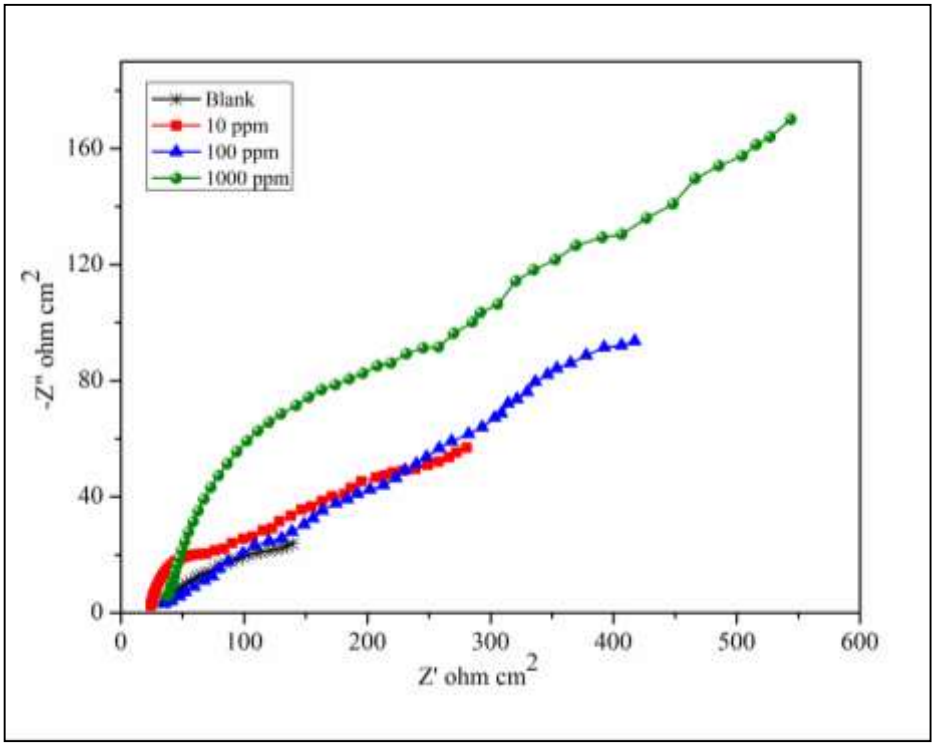

Fig. 7.5 Nyquist plot for selected concentrations of MPOU in simulated concrete pore solution

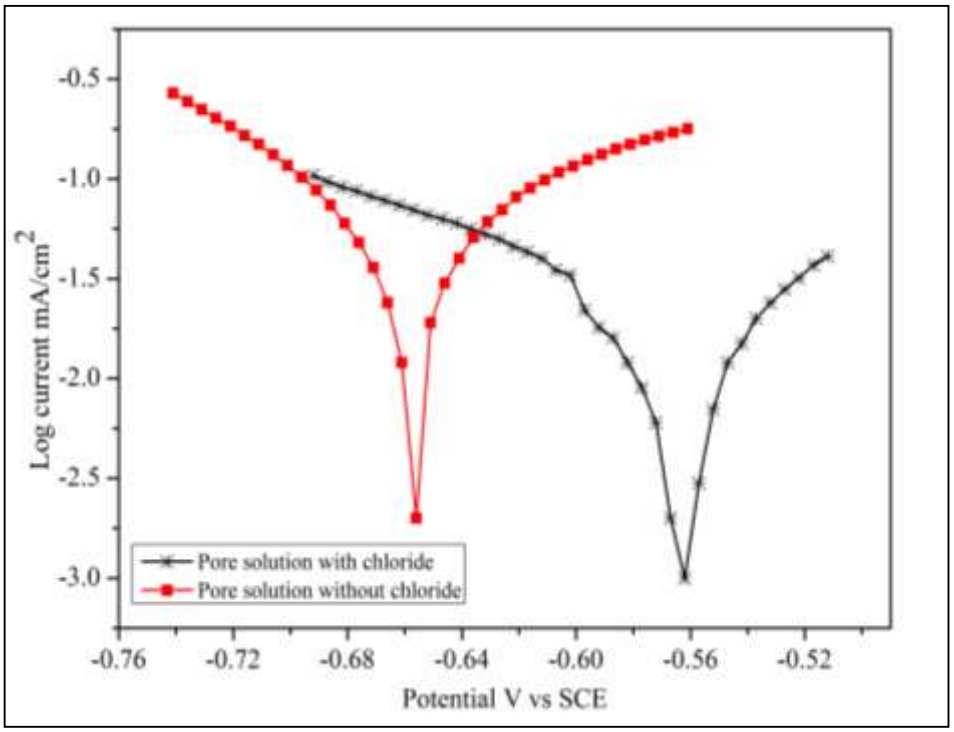

Fig. 7.6 Polarisation curves for pore solution in the absence and presence of chloride ions

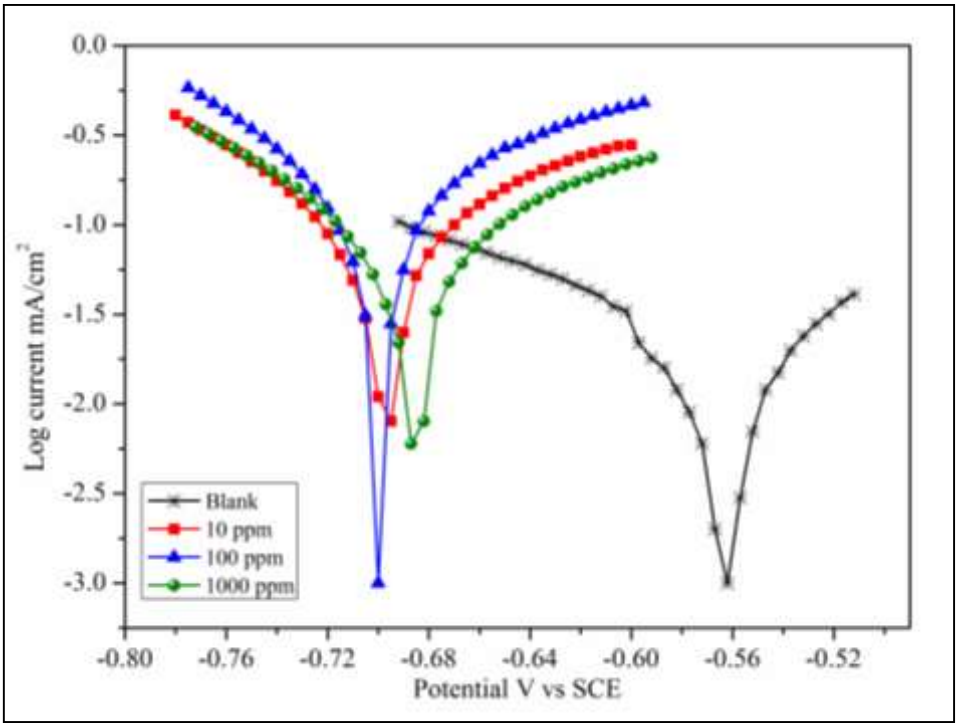

Fig. 7.7 Polarisation curves for selected concentrations of PGAZ in simulated concrete pore solution

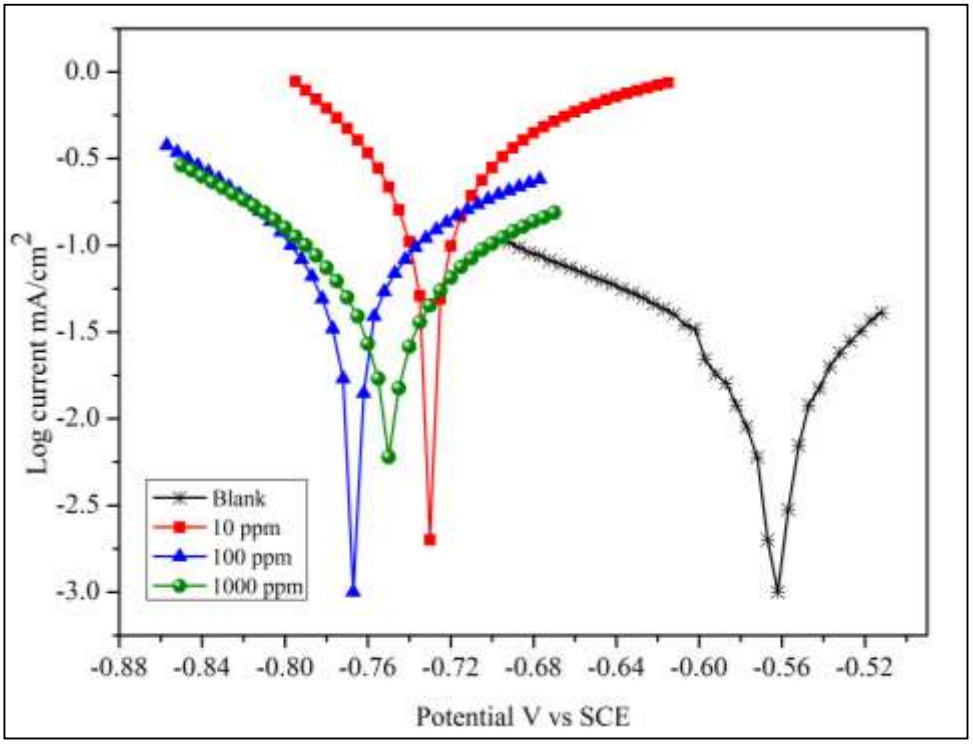

Fig. 7.8 Polarisation curves for selected concentrations of PGSE in simulated concrete pore solution

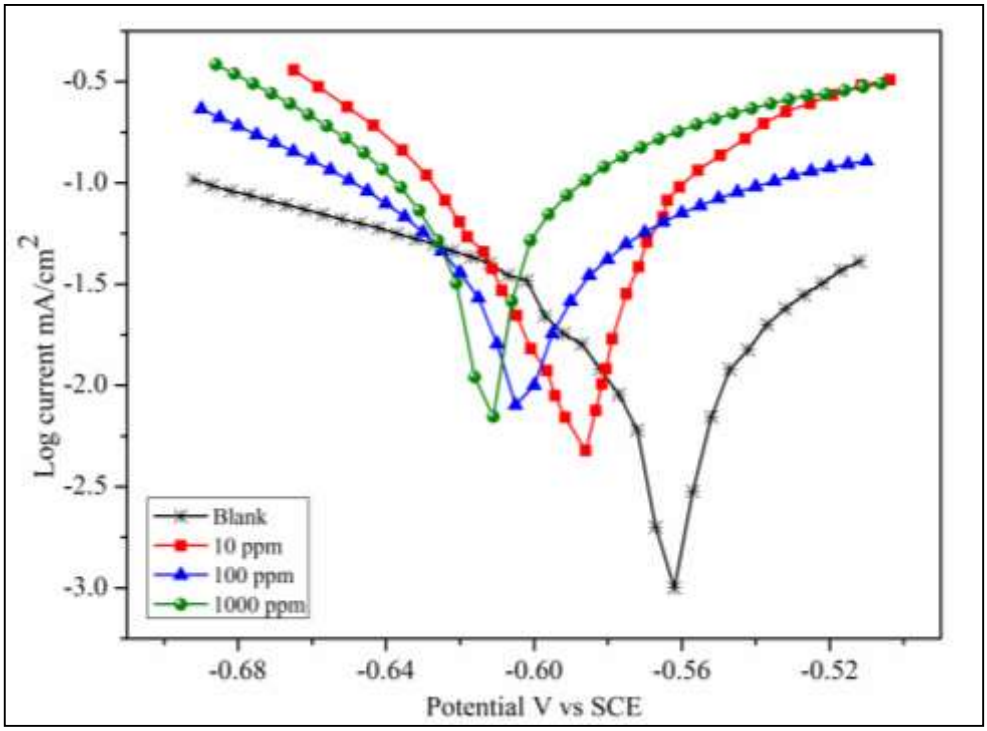

Fig. 7.9 Polarisation curves for selected concentrations of MPOD in simulated concrete pore solution

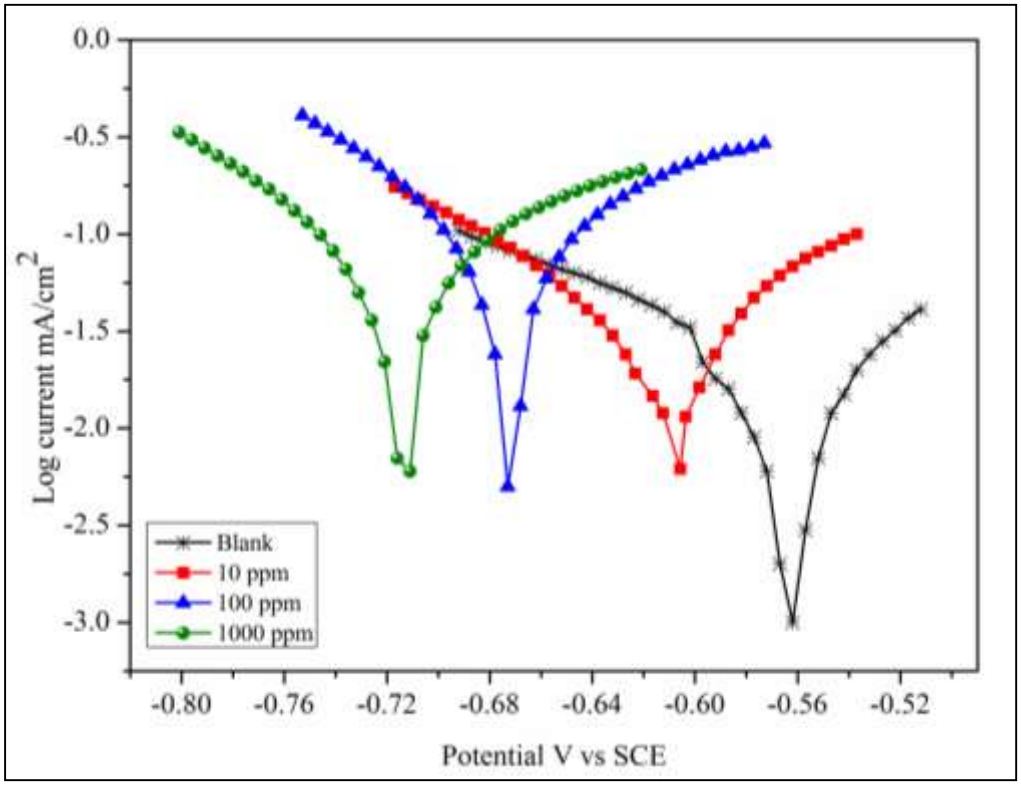

Fig. 7.10 Polarisation curves for selected concentrations of MPOU in simulated concrete pore solution

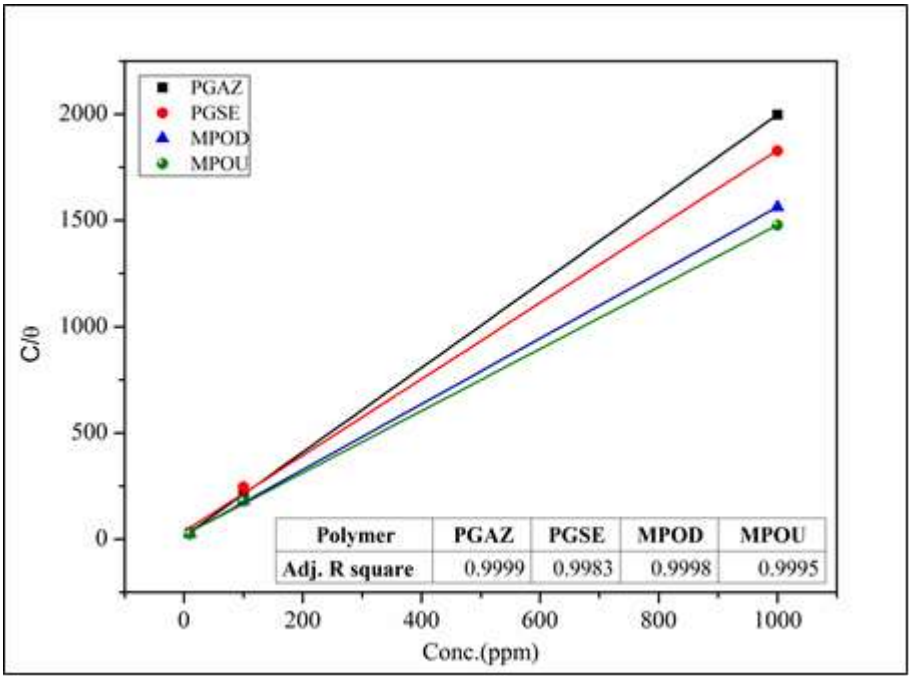

Fig. 7.11 Langmuir adsorption isotherm plot for selected concentrations of the polyesters

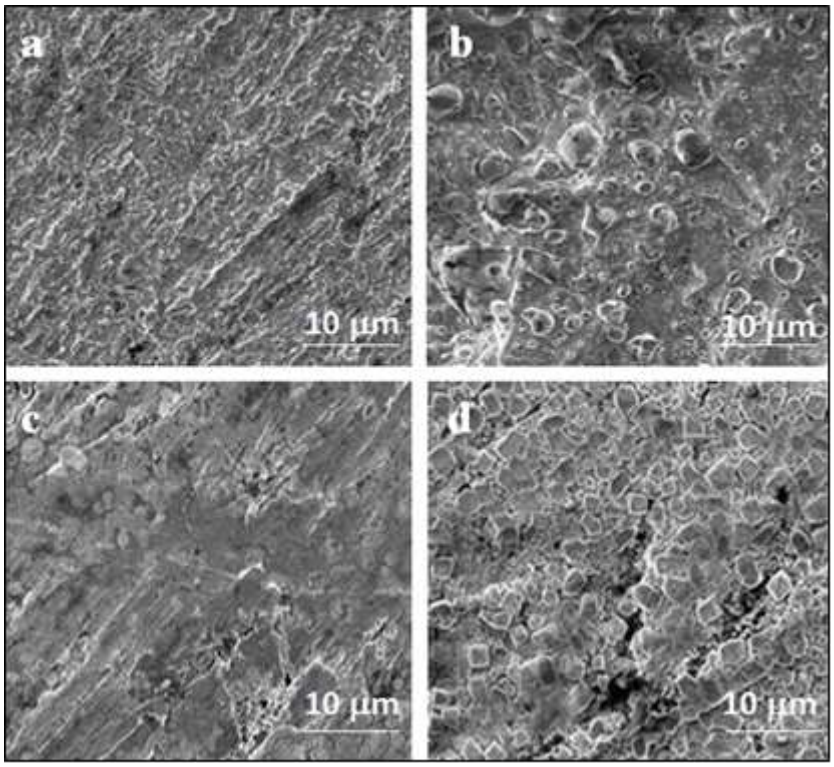

Fig. 7.12 SEM images for rebar in a) absence of chloride ions b) presence of chloride ions c) presence of PGAZ d) presence of MPOD.

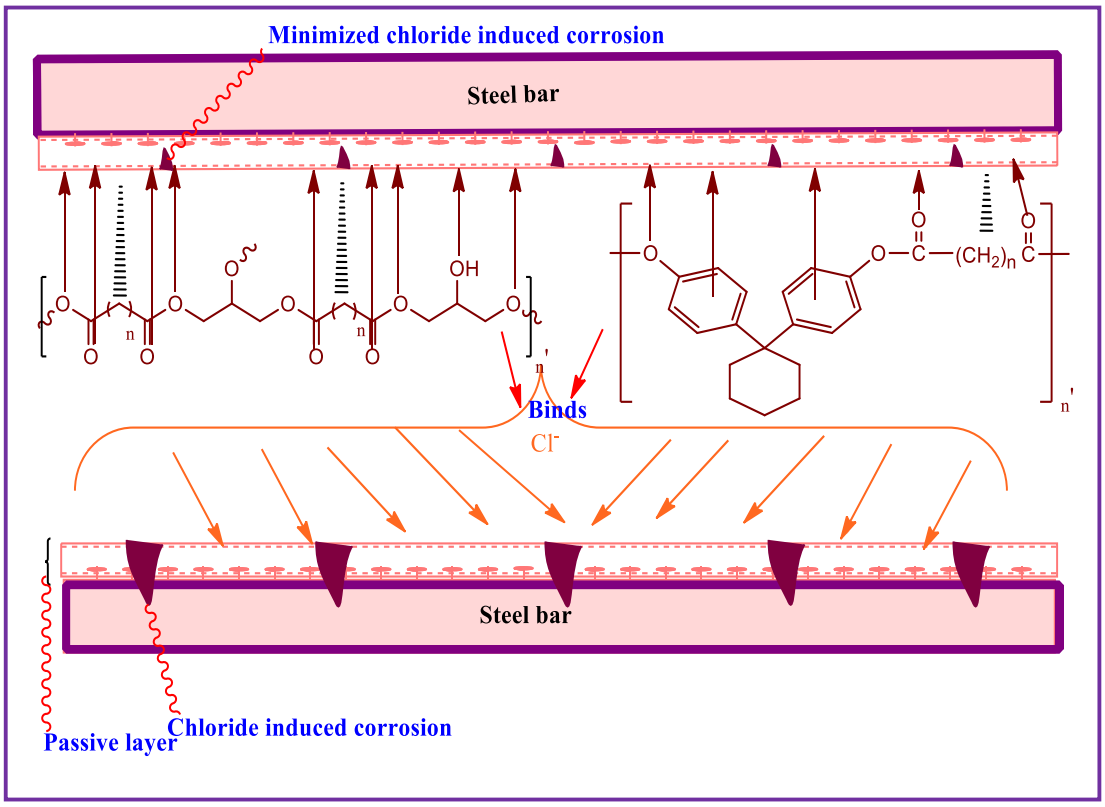

Fig. 7.13 Schematic representation of proposed mechanism